1-4-2005

Endothelial-Specific Expression of Caveolin-1 Impairs Microvascular Permeability and Angiogenesis

Philip M. Bauer
Yale University

Jun Yu
Yale University

Yan Chen
Yale University

Reed Hickey
Yale University

Pascal N. Bernatchez
Yale University

See next page for additional authors

Endothelial-specific expression of caveolin-1 impairs microvascular permeability and angiogenesis

Philip M. Bauer*, Jun Yu*, Yan Chen*, Reed Hickey†, Pascal N. Bernatchez*, Robin Looft-Wilson*, Yan Huang†, Frank Giordano†, Radu V. Stan‡, and William C. Sessa*§

*Departments of Pharmacology and Vascular Cell Signaling and Therapeutics Program, Boyer Center for Molecular Medicine, and †Medicine and Cardiovasculate Gene Therapy Program, Yale University School of Medicine, New Haven, CT 06536; and ‡Department of Pathology, Dartmouth Medical School, Lebanon, NH 03756

Edited by Louis J. Ignarro, University of California School of Medicine, Los Angeles, CA, and approved November 22, 2004 (received for review August 18, 2004)

The functions of caveolae and/or caveolins in intact animals are beginning to be explored. Here, by using endothelial cell-specific transgenesis of the caveolin-1 (Cav-1) gene in mice, we show the critical role of Cav-1 in several postnatal vascular paradigms. First, increasing levels of Cav-1 do not increase caveolae number in the endothelium *in vivo*. Second, despite a lack of quantitative changes in organelle number, endothelial-specific expression of Cav-1 impairs endothelial nitric oxide synthase activation, endothelial barrier function, and angiogenic responses to exogenous VEGF and tissue ischemia. In addition, VEGF-mediated phosphorylation of Akt and its substrate, endothelial nitric oxide synthase, were significantly reduced in VEGF-treated Cav-1 transgenic mice, compared with WT littermates. The inhibitory effect of Cav-1 expression on the Akt-endothelial nitric oxide synthase pathway was specific because VEGF-stimulated phosphorylation of mitogen-activated protein kinase (ERK1/2) was elevated in the Cav-1 transgenics, compared with littermates. These data strongly support the idea that, *in vivo*, Cav-1 may modulate signaling pathways independent of its essential role in caveolae biogenesis.

nitric oxide | caveolae | VEGF | signal transduction

Caveolae are 50- to 100-nm flask-shaped invaginations of the plasma membrane (1) and are present in most mammalian cells. The putative functions of caveolae include cholesterol transport (2, 3), endocytosis (4), potocytosis (5), and signal transduction (6–9). Recent insights into the physiological roles of caveolae and their primary coat proteins, caveolins, have been dissected in genetically modified mice (10, 11). Caveolin-1 (Cav-1) and Cav-3 are dispensable during vascular and organ development but are essential for caveolae formation in specialized cells including most endothelia, adipocytes, and skeletal/cardiac myocytes. *In vitro* data have shown that signaling molecules can potentially interact with Cav-1, and that interactions with Cav-1 can increase or decrease the fidelity or magnitude of signaling (12–14). The ability of proteins to localize in caveolae, in addition to direct interactions of proteins with caveolins, has led to the hypothesis that caveolae may compartmentalize signaling in the plasma membrane and that the interactions (direct and indirect) between resident proteins and Cav-1 may fine-tune the signaling cascades.

Physiologically, the loss of caveolae results in impairment of cholesterol homeostasis (15), insulin sensitivity (16), nitric oxide (NO) (10, 11), calcium signaling (10), and cardiac function (17). These studies validate the *in vivo* importance of caveolae and caveolins beyond cell-based studies that are largely hampered by operational definitions of biochemical fractions containing caveolins and the lack of specificity inherent in reagents that remove cellular cholesterol. Although caveolin knockout mice are useful to delineate the importance of caveolae in a given response, there are additional questions that are difficult to dissect, because the loss of Cav-1 and Cav-3 abolishes both the caveolae organelle as well as the pathways regulated by protein–protein or protein–lipid interactions with the caveolins. To study how Cav-1 influences cardiovascular signaling in mice replete with caveolae, we generated mice that overexpress Cav-1 in the endothelial layer of blood vessels and examined different aspects of vascular cell signaling and angiogenesis.

Materials and Methods

Generation of Endothelial-Specific Cav-1 Transgenic (TG) Animals. Cav-1 TG mice were generated as described in ref. 18. Briefly, canine Cav-1 was subcloned into the *Not*I site of the PEP8 plasmid vector consisting of the pCDM8 backbone (Invitrogen), the 9.2-kb murine preproET-1 5′ flanking promoter, the SV40 intron poly(A) signal, and a single *Not*I site by using standard techniques. The plasmid, or PEP-Cav-1, was purified on a cesium chloride/ethidium bromide gradient. The plasmid was linearized by *Spe*I digestion and subjected to agarose gel electrophoresis. The linearized plasmid was then electroeluted from the gel, and DNA was used to generate TG mice by using standard techniques.

Immunohistochemistry. Eight- to 10-week-old Cav-1 TG or WT littermates were perfused with PBS for 5 min and then with 4% paraformaldehyde for 5 min at physiological temperature and pressure. Blood vessels were then harvested and diffusion-fixed overnight at 4°C and then dehydrated in 30% sucrose overnight at 4°C. The vessels were then embedded, and 5-μm sections were stained for Cav-1. Cav-1 was visualized by using the VECTASTAIN ABC kit (Vector Laboratories), followed by incubation with NovaRed substrate (Vector Laboratories).

EM. Cav-1 TG mice or WT littermates were perfused for 10 min at room temperature (RT) under anesthesia with oxygenated DMEM through the left ventricle, followed by fixation by perfusion (10 min at RT) with 2.5% glutaraldehyde and 3% paraformaldehyde in 0.1 M sodium cacodylate buffer (pH 7.3). Specimens were taken from different tissues and trimmed into small blocks. The blocks were immersed into fresh fixative (1 h at RT), washed twice (15 min at RT) in 0.1 M cacodylate, postfixed in Palade's OsO_4 (1 h on ice), *en bloc*-stained in Kellemberger's uranyl acetate (overnight at RT), dehydrated in graded ethanol, and embedded in LX112 resin (Ladd Research Industries, Burlington, VT). Thin sections (50 nm) were cut, stained with lead citrate, and examined and photographed under an electron microscope (JEOL 1200EX or CM10, Phillips Electronic Instruments, Mahwah, NJ). Caveolae number per μm of endothelial cell length was determined by counting the number of plasmalemmal attached caveolae from 50 sections per animal per tissue ($n = 3$ mice per group).

This paper was submitted directly (Track II) to the PNAS office.

Abbreviations: TG, transgenic; Cav, caveolin; NO, nitric oxide; eNOS, endothelial NO synthase; PE, phenylephrine; ACh, acetylcholine; L-NAME, L-nitro arginine methyl ester; RT, room temperature; PECAM, platelet-endothelial cell adhesion molecule.

§To whom correspondence should be addressed. E-mail: william.sessa@yale.edu.

www.pnas.org/cgi/doi/10.1073/pnas.0406092102

Aortic-Ring Assay. The thoracic aorta is dissected from male mice (8–10 weeks old) and cut into cylindrical, 3-mm-long segments. The rings are suspended by two tungsten wires mounted in a vessel myograph system (Danish Myotechnologies, Aarhus, Denmark). The aortas were bathed in oxygenated Krebs buffer and submitted to a resting tension of 9.8 mN. After 60 min of equilibration with frequent washings, concentration response curves for phenylephrine (PE) were generated to determine vasoconstrictor responses. To study vasodilator and L-nitro arginine methyl ester (L-NAME) responses, the rings were preconstricted with a submaximal concentration of PE, and acetylcholine (ACh) (10^{-9} to 10^{-5} M), sodium nitroprusside (SNP) (10^{-9} to 3×10^{-7} M), or L-NAME (100 μM) was injected at the plateau of the PE-induced contraction.

***In Vivo* Microvessel Pharmacology.** In second-order branches off the major vessel entering the cremaster muscle (2A arterioles), vasoconstriction to PE (10^{-9} to 10^{-4} M), and vasodilation to ACh (10^{-9} to 10^{-4} M), bradykinin (10^{-9} to 10^{-5} M), and isoproteronol (10^{-10} to 10^{-5} M) were measured *in vivo* by using intravital microscopy (19). Arteriolar internal diameter was measured by video microscopy (resolution ± 2 μm). Agonist-induced diameter changes were tested in semirandom order by cumulative addition to the superfused physiological salt solution (137 mM NaCl/4.7 mM KCl/1.2 mM $MgSO_4$/2 mM $CaCl_2$/18 mM $NaHCO_3$, equilibrated with 5% CO_2/95% N2) with at least 2 min between each dose.

Immunoprecipitation and Western Blot. Tissues for Western blot analysis were flash-frozen, crushed, and resuspended in lysis buffer [50 mM Tris·HCl, pH 7.4/100 mM NaCl/0.1 mM EGTA/0.1 mM EDTA/1% Triton X-100/1 mM sodium orthovanadate/20 mM NaF/1 mM $Na_4P_2O_7$/1 mM Pefabloc SC and protease inhibitor mixture (Roche Diagnostics); for Cav-1 immunoprecipitation; 10 mM Tris, pH 8.0/60 mM *n*-octyl β-D-glucopyranoside/150 mM NaCl/1 mM sodium orthovanadate/20 mM NaF/1 mM $Na_4P_2O_7$/1 mM Pefabloc/10 μg/ml aprotinin/10 μg/ml leupeptin]. Insoluble material was removed by centrifugation at $12{,}000 \times g$ for 10 min at 4°C. Fifty micrograms of protein from cell lysates was then analyzed by Western blot analysis, or 500 μg of protein from lysates was immunoprecipitated for Cav-1 or VEGF receptor 2 (VEGFR2) and subjected to Western blot analysis.

Modified Mile's Assay. Mice were anesthetized with ketamine/xylazine (60 mg/kg/15 mg/kg i.m.), and a catheter was introduced into the left jugular vein for administration of Evans blue (30 mg/kg; Sigma). One minute after the administration of the dye, VEGF (30 ng in 30 μl) or saline was injected into the right and left dorsal ear skin, respectively. After 30 min, the animals were killed and perfused, and the ears were removed, dried in an oven at 55°C, and weighed. Evans blue content of the ear was evaluated by extraction with 500 μl of formamide for 24 h at 55°C and measured spectrophotometrically at 610 nm. Results were compared with a standard curve of Evans blue in formamide.

Ear Angiogenesis. Ear angiogenesis studies are described in ref. 20. An adenovirus vector encoding murine VEGF-A164 (AdVEGF; 10^8 plaque-forming units in 15 μl) was injected s.c. into the ears of 8- to 12-week-old male mice. Contralateral ears were injected with an adenovirus encoding green fluorescent protein (AdGFP). After 6 days, mice were killed and the ears were removed and embedded. Frozen sections (5 μm) were immunostained with an antibody against the endothelial-cell marker PECAM (platelet-endothelial cell adhesion molecule) and quantified by immunofluorescence.

Hind-Limb Ischemia. Male mice (8–10 weeks old) were anesthetized with ketamine/xylazine (60 mg/kg/15 mg/kg i.m.), and a skin incision was made on the inside of the hind limb to expose the muscles of the upper and lower hind limb. The proximal femoral artery including the superficial and deep branch and the distal portion of the saphenous artery were ligated and dissected. Flow was measured in the muscle of the lower limb of the ischemic (left leg) and nonischemic (right leg) mice by placing a deep laser Doppler probe directly on the gastrocnemius muscle. This probe penetrates 1 mm into the tissue and measures blood flow throughout the muscle. Flow measurements were made before and imme-

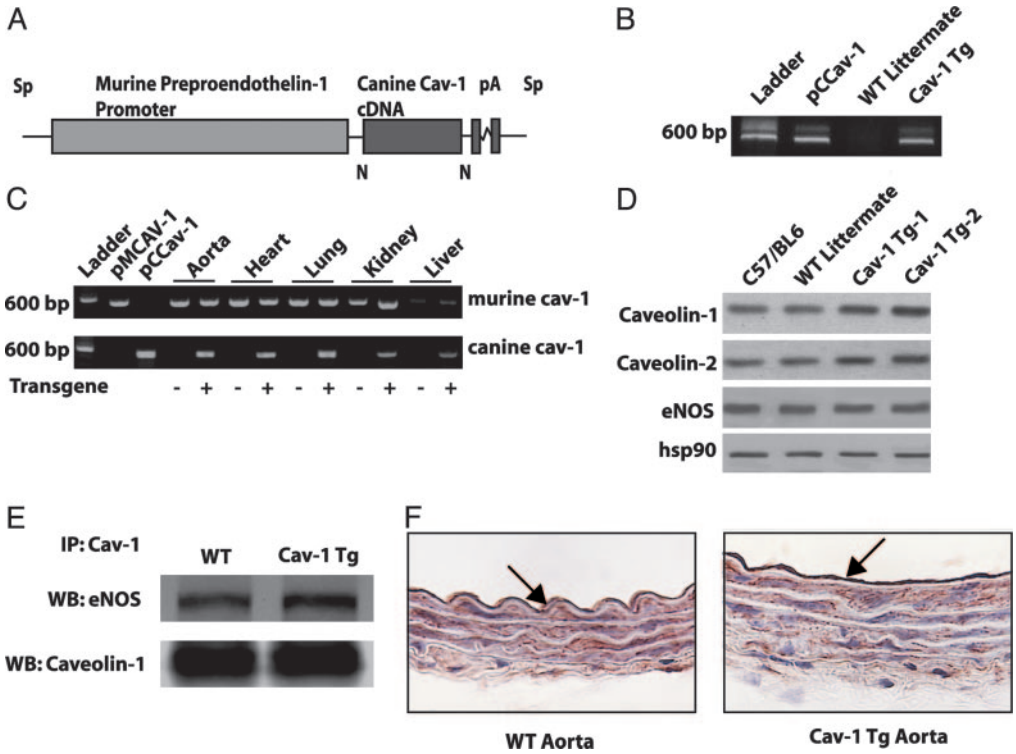

Fig. 1. Generation of endothelium-specific TG mice. (*A*) Construct used for generating the Cav-1 TG mice. The canine Cav-1 cDNA was driven by the preproendothelin promoter. (*B*) Expression of the transgene vs. endogenous Cav-1. Primers specific for canine Cav-1 recognize the plasmid containing canine Cav-1 (pCCav-1) and TG Cav-1 (Cav-1 TG) but not endogenous Cav-1 (WT littermate). (*C*) The presence of both WT and transgene Cav-1 by RT-PCR in various tissues. pMCav-1 is the murine Cav-1 cDNA (*D*) The increased expression of Cav-1 and Cav-2 in aortic extracts from two TG lines (TG-1 and TG-2), compared with C57Bl6 or WT littermates. (*E*) Immunoprecipitation of Cav-1 from TG lung extracts increases the amount of eNOS co-associated (*Lower*, total Cav-1 immunoprecipitated; *Upper*, coassociated eNOS). (*F*) Immunohistochemical evidence for expression of Cav-1 transgene in the endothelium. WT and Cav-1 TG aortic sections were stained with a Cav-1 mAb. Note the presence of intense labeling of Cav-1 in the EC, with little difference in the intensity of Cav-1 in underlying smooth muscle.

diately after surgery, then again at 2 and 4 weeks postsurgery. Skeletal muscle isolated from the ischemic leg 4 weeks after femoral ligation was fixed with methanol and then embedded in paraffin. Multiple sections (5 μm) were stained for PECAM-1 (Pharmingen) and visualized by using the VECTASTAIN ABC kit followed by incubation with NovaRed substrate (Vector Laboratories).

Assessment of *in Vivo* Phosphorylation. Male mice (8–12 weeks old) were anesthetized with ketamine/xylazine (60 mg/kg/15 mg/kg i.m.), and a catheter was introduced into the left jugular vein for administration of VEGF. Either human $VEGF_{165}$ (2 mg) or saline was injected and allowed to circulate for 5 min. The animal was then perfused with 5 ml of PBS supplemented with phosphatase inhibitors (1 mM sodium orthovanadate/20 mM NaF/1 mM $Na_4P_2O_7$), after which the lungs were harvested for Western blot analysis.

Results and Discussion

Cav-1 TG mice were generated by using *Spe*I-linearized prepro-endothelin-1 promoter to drive the Cav-1 transgene (Fig. 1*A*) (18). Founder mice harboring the transgene were identified by PCR of genomic DNA isolated from tail biopsies at age 3–4 weeks (Fig. 1*B*). Fourteen founders were independently bred to C57BL/6J mice to assess stable transmission of the transgene. Eight founders stably transmitted the transgene after three rounds of backcrossing to C57BL/6J mice. All experiments were performed with heterozygous Cav-1 TG mice and their non-TG littermates as controls. There were no apparent morphological abnormalities in Cav-1 TG mice. The mice had normal body weights, heart-to-body weight ratios, heart rates, and blood pressure (Table 1), and serum NO levels (measured as NOx) in the Cav-1 TG mice were not significantly different from those in WT mice. Male and female mice appeared equally fertile, and there were no differences in grooming behavior or growth rate, compared with WT littermates.

RT-PCR to detect canine Cav-1 mRNA revealed transgene expression in the heart, lung, aorta, brain, and liver of Cav-1 TG but not WT mice (Fig. 1*C*). Western blot analysis revealed that Cav-1 is 2-fold overexpressed in aorta of the Cav-1 TG mice from two different founders bearing the Cav-1 transgene (Fig. 1*D*). Additionally, Cav-2 is up-regulated in the Cav-1 TG mice, consistent with data indicating that expression of Cav-1 is important for the stability of Cav-2 (Fig. 1*D*) (10, 11). It is important to note that the relative overexpression of Cav-1 in the endothelium is greater than can be demonstrated by Western blot analysis because the endothelium is a single cell layer, compared with several layers of smooth muscle, which also express Cav-1. Endothelial NO synthase (eNOS) levels were not changed in the Cav-1 TGs, compared with WT littermates (Fig. 1*D*), however, more eNOS was associated with Cav-1 in the Cav-1 TGs as assessed by coimmunoprecipitation of eNOS with Cav-1 isolated from lung extracts (Fig. 1*E*). Immunohistochemical staining of aorta revealed overexpression of the transgene in the endothelium of Cav-1 TG mice (Fig. 1*F*), whereas staining for Cav-1 in the smooth muscle layer is similar between Cav-1 TGs and WT littermates.

Cav-1 is responsible for caveolae biogenesis in the endothelium *in vivo*, because these organelles are absent in mice deficient in Cav-1 (10, 11). Thus, we quantified caveolae number in the heart and aorta from WT and Cav-1 TG mice. Transmission electron micrographs were collected, and caveolae attached to the luminal and abluminal plasma membranes of endothelial cells were quantified. Fig. 2*A* shows electron micrographs of coronary capillaries from WT and Cav-1 TG mice and quantification of caveolae number in coronary capillaries (Fig. 2*B*). Interestingly, there were no significant difference in caveolae number in Cav-1 TG mice, compared with WT littermates. Qualitatively similar results were obtained in aorta and coronary arterioles (data not shown). These data *in vivo* are unlike studies in cultured cells (which have 100-fold fewer caveola per μm of membrane) where acute overexpression of Cav-1 increases caveolae number (21–25). Thus, *in vivo*, the number of endothelial caveola in the endothelia of vessels examined appears maximal, and organelle number is not regulated by further increases in Cav-1 protein levels.

Table 1. Baseline parameters and hemodynamics of wild-type littermates and Cav-1 TG mice

	WT		Cav-1 TG	
	Mean	SEM	Mean	SEM
Body weight, g	26.43	0.46	24.98	0.57
Heart, mg/body weight, g	4.90	0.18	5.05	0.11
MAP, mmHg*	105.38	6.03	103.02	5.26
Heart rate, beats per min	207.75	12.07	204.83	14.30
Plasma NOx, mM	15.28	1.30	13.54	0.54

Data are mean ± SEM, with $n = 9$ per group.
*1 mmHg = 133 Pa.

Next, we examined whether overexpression of Cav-1 regulates vascular functions. Because there is biochemical and genetic support for eNOS regulation by a direct interaction with Cav-1 (14, 26, 27), we examined the effect of endothelial Cav-1 overexpression on eNOS function in large blood vessels by quantifying the vascular reactivity of aortic rings to the endothelium-dependent vasodilator ACh and to the NOS inhibitor L-NAME. Consistent with Cav-1 being an endogenous inhibitor of eNOS activity, aorta from Cav-1 TG mice were less responsive to ACh. Fig. 3*A* shows typical experimental traces of aortic rings from WT and Cav-1 TG mice. Higher concentrations of ACh are required to elicit relaxation of the isolated aorta. Analysis of the dose–response relationships in the two strains reveals that the EC_{50} is shifted nearly 10-fold in the Cav-1 TG animals (EC_{50} in WT aorta = $4.91 \pm 0.06 \times 10^{-8}$M; EC_{50} in Cav-1 TG aorta = $3.93 \pm 0.05 \times 10^{-7}$M) (Fig. 3*B*). In addition, basal NO release in Cav-1 TG mice also was diminished, as depicted in the trace in Fig. 3*C*. Vessels were preconstricted with a submaximal dose of PE, and the NOS inhibitor L-NAME (100 μM) was added at the peak of the constriction to remove endogenous NO.

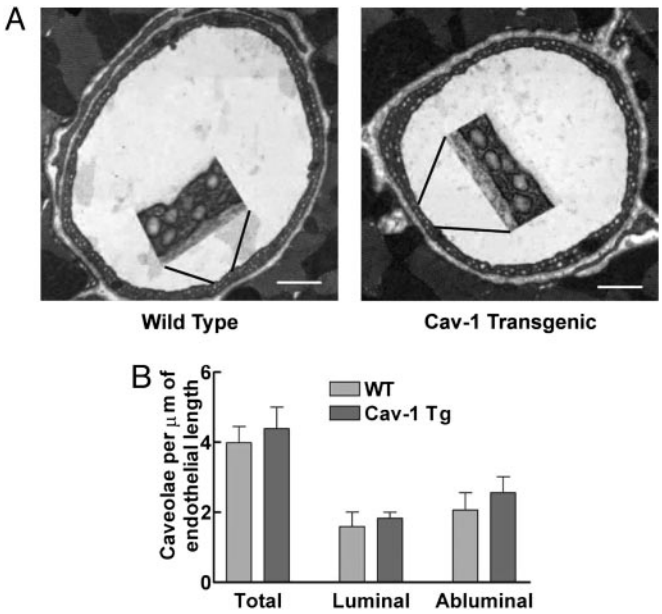

Fig. 2. TG expression of Cav-1 in endothelium does not change caveolae number. (*A*) Representative transmission electron micrographs of coronary capillaries from WT or TG mice. (*Insets*) Magnifications (×4) to demonstrate the caveolae anatomy. (Scale bar: 1 μm.) (*B*) Quantification of luminal and abluminal caveolae structures. Data (mean ± SEM) are from 50 sections per mouse with $n = 3$ mice per group.

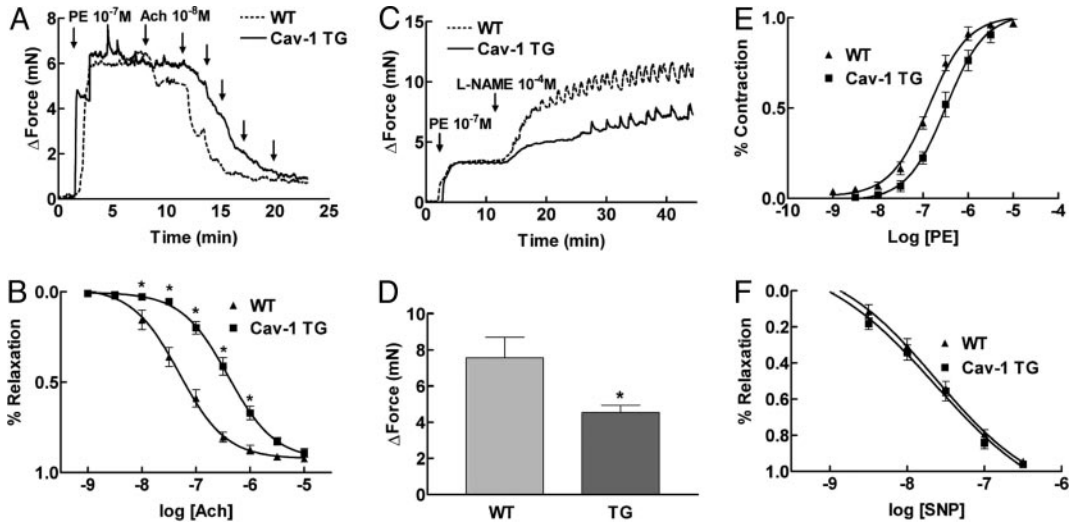

Fig. 3. Endothelial expression of Cav-1 impairs eNOS-dependent vasodilation. (*A*) Representative bioassay trace from WT littermate (intermittent line) and Cav-1 TG (solid line) mice. Aortic rings were precontracted with PE, and ACh-induced dilations were examined. (*B*) Statistical analysis of the full dose–response curves to ACh demonstrates a 10-fold change in the EC_{50} value for ACch in Cav-1 TG mice. (*C*) Basal eNOS activation is reduced in Cav-1 TG. Vessels were contracted with PE and then incubated with a NOS inhibitor L-NAME to remove basal NO synthesis. (*D*) Cav-1 TG mice show a deficiency in basal NO synthesis. (*E* and *F*) The deficit in eNOS activation does not influence the ability of the vessels to contract to PE or to relax to the NO donor drug, SNP. Data are mean ± SEM, with $n = 5$ animals and two aortic rings per animal. *, $P < 0.05$.

L-NAME caused a further constriction of WT vessel, resulting in an increase in isometric tension reflecting the removal of basally released NO. However, constriction of the vessel in response to L-NAME was significantly attenuated in Cav-1 TG mice (Fig. 3*D*). These effects on vasomotion occur selectively in the endothelium because the vasoconstrictor action of PE and the NO donor drug SNP elicit similar responses in the two strains (Fig. 3 *E* and *F*). Collectively, these data support the idea that a major role of Cav-1 in endothelium is to regulate eNOS function.

In contrast, when using intravital microscopy to determine the vascular reactivity of small arterioles (100 μm or less) in the cremaster muscle, there were no differences in the diameters or responsiveness of the microcirculatory bed to standard pharmacological stimuli between the two strains (Table 2). These results are not surprising, because it is recognized that other pathways (such as endothelial-derived hyperpolarizing factor signaling through gap-junctional coupling) are the predominate vasodilatory pathways in the mouse microcirculation (28, 29).

The role of Cav-1 or caveolae in regulating vascular barrier function and permeability is not well understood. Caveolae are highly abundant in capillaries and in postcapillary venules. In Cav-1(−/−) mice, the loss of caveolae results in reduced steady-state plasma albumin levels and increases in the clearance of radioactive albumin, suggesting that the vessels are hyperpermeable (30). To assess whether Cav-1 can influence vascular leakage, we examined the ability of VEGF to induce the extravasation of Evans blue in the ears of WT vs. Cav-1 TG mice. Mice were injected i.v. with Evans blue (which binds to plasma albumin), and the dye was allowed to circulate for 5 min. VEGF (30 ng) was then injected into the right ear of the mouse, and saline was injected into the left ear. After 30 min, mice were killed, and Evans blue extravasation into the interstitium was quantified. As illustrated in Fig. 4*A*, Cav-1 overexpression reduces VEGF-stimulated Evans blue extravasation into the ear interstitium, compared with responses in WT littermates. Thus, endothelial-specific Cav-1 overexpression reduced VEGF-stimulated vascular permeability, presumably by attenuating eNOS-dependent blood flow and/or permeability changes evoked by the angiogenic cytokine.

Table 2. EC_{50} determined by intravital microscopy in the cremaster muscle

	WT		Cav-1 TG	
	Mean	SEM	Mean	SEM
Phenylephrine	1.50×10^{-6}	6.20×10^{-7}	2.97×10^{-6}	1.20×10^{-6}
Acetylcholine	7.40×10^{-6}	3.34×10^{-6}	5.67×10^{-6}	2.14×10^{-6}
Bradykinin	4.69×10^{-7}	2.01×10^{-7}	7.14×10^{-7}	3.70×10^{-7}
Isoproterenol	3.82×10^{-9}	5.53×10^{-10}	1.21×10^{-9}	3.05×10^{-10}

Potency of vasoconstrictors (phenylephrine) and vasodilators (acetylcholine, bradykinin, and isoproterenol) in the microcirculation of WT littermates and Cav-1 TG mice. Data are mean ± SEM, with $n = 7$ per group.

Considering that VEGF-mediated vascular permeability is a key component of the angiogenic process *in vivo*, we assessed whether expression of Cav-1 influenced angiogenesis. WT and Cav-1 TG mice were injected with equal multiplicity of infection of adenoviral adVEGF164 into the right ear and, as a control, AdGFP into the left ear. After 6 days, the extent of angiogenesis was determined through staining for the endothelial marker, PECAM-1. Fig. 4*B* shows greater density of PECAM-1-labeled structures in WT mice, compared with Cav-1 TG mice. Quantification of the extent of angiogenesis shows that Cav-1 overexpression reduces VEGF-mediated angiogenesis by 40%, compared with littermate controls (Fig. 4*C*).

Recent studies suggest that localization of VEGFR2 to caveolae may be an important factor in VEGF-induced signaling (31). To determine whether the lack of VEGF-driven permeability and angiogenesis were due to defects in VEGF-induced signaling pathways, we determined the *in vivo* phosphorylation of targets downstream of VEGFR activation. Age-matched littermates and Cav-1 TG mice were injected i.v. with VEGF (2 mg). After 5 min, lungs were excised and processed for semiquantitative Western blot analysis (32). As seen in Fig. 4*D*, VEGF stimulated the tyrosine phosphorylation of the endothelial VEGFR, VEGFR2, in both WT and Cav-1 TG mice, suggesting that impairment of signaling in Cav TG mice is not a direct effect on VEGFR2 localization or dimerization (Fig. 4*D*). In contrast, VEGF-mediated phosphorylation of the protein kinase Akt (on serine 473) and the Akt substrate, eNOS (on serine 1179), was significantly reduced in VEGF-treated Cav-1 TG mice, compared with littermate controls. The inhibitory effect

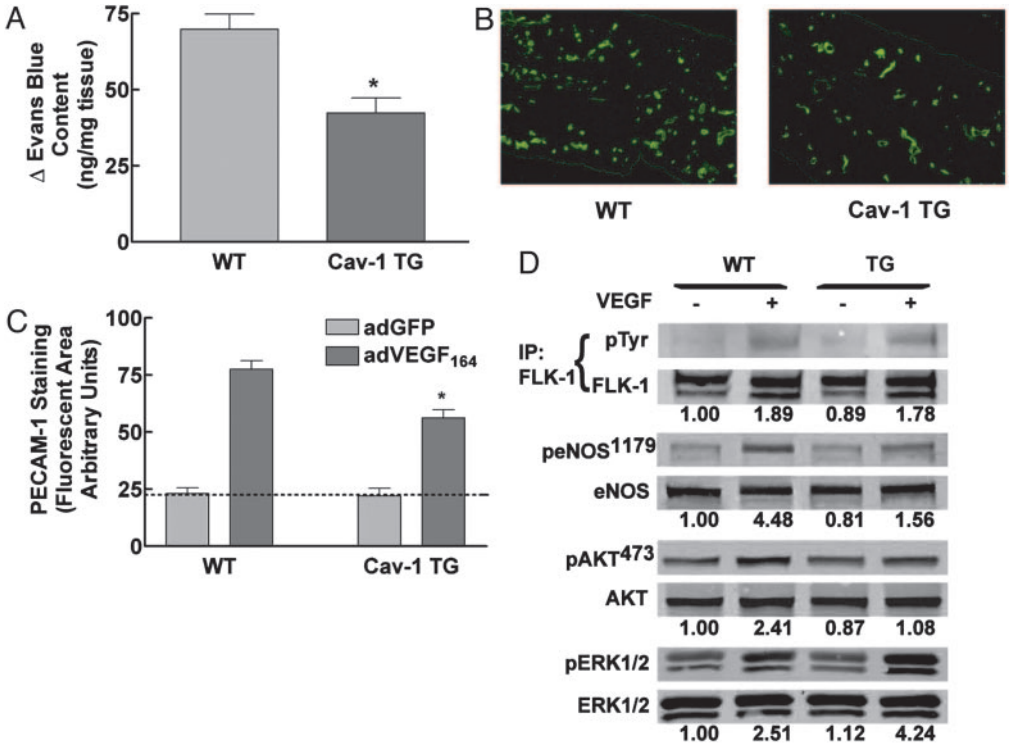

Fig. 4. VEGF-mediated functions are reduced in Cav-1 TG mice. (*A*) Cav-1 TG mice exhibit reduced (30 min) VEGF-stimulated vascular leakage. Data are mean ± SEM ($n = 6$). (*B*) PECAM-1-positive vascular structures in the ears of WT (*Left*) or Cav-1 TG (*Right*) mice injected with AdVEGF (after 6 days). (*C*) AdVEGF-mediated angiogenesis was reduced in Cav-1 TG (mean ± SEM, with $n = 6$ animals per group, and 10 fields were quantified for each ear). (*D*) VEGF-mediated signal transduction to Akt and eNOS are reduced in Cav-1 TG mice. Mice were injected with saline or VEGF, and lung tissue was processed for Western blot analysis. The numbers below represent densitometric evaluation of the data, with a value of 1.0 reflecting the basal level of phosphorylation of each signaling protein (FLK, eNOS, Akt, and ERK, respectively). Similar results were obtained in three additional experiments. *, $P < 0.05$.

of Cav-1 expression on the Akt-eNOS pathway was specific, because VEGF-stimulated phosphorylation of ERK1/2 was not reduced but enhanced in the Cav-1 TGs, compared with littermates. This suggests that, in endothelial cells, Cav-1 differentially regulates VEGF-induced signal transduction, and that diminution of the Akt/eNOS axis provides a plausible mechanism to explain the defects in vasodilation, permeability, and angiogenesis in this model. Finally, as an independent assay to determine the role of endothelial Cav-1 in angiogenesis, we induced tissue ischemia in the hind limb of WT littermates and Cav-1 TG mice. In this model, ligation of the left femoral artery triggers tissue ischemia followed by an increase in arteriogenesis and angiogenesis (33). After surgery, blood flow was reduced to the same extent in the ischemic legs of WT littermate mice and Cav-1 TG. However, blood flow recovery, reflecting arteriogenesis and angiogenesis, was significantly reduced at 2 and 4 weeks postsurgery in Cav-1 TG mice (Fig. 5*A*). To quantify the clinical differences between the Cav-1 TG and WT littermates, a clinical score index between 0 and 4 was assigned to each mouse (Fig. 5*B*). Immediately after surgery, the clinical score of both groups was 1, indicating that the mice had gait abnormalities and paleness of the foot due to lack of blood flow. WT mice mostly recovered by 2 weeks and had a clinical score of 0 by 4 weeks, indicating complete recovery. All of the Cav-1 TG mice had a clinical score of 2 by 2 weeks, indicating partial necrosis

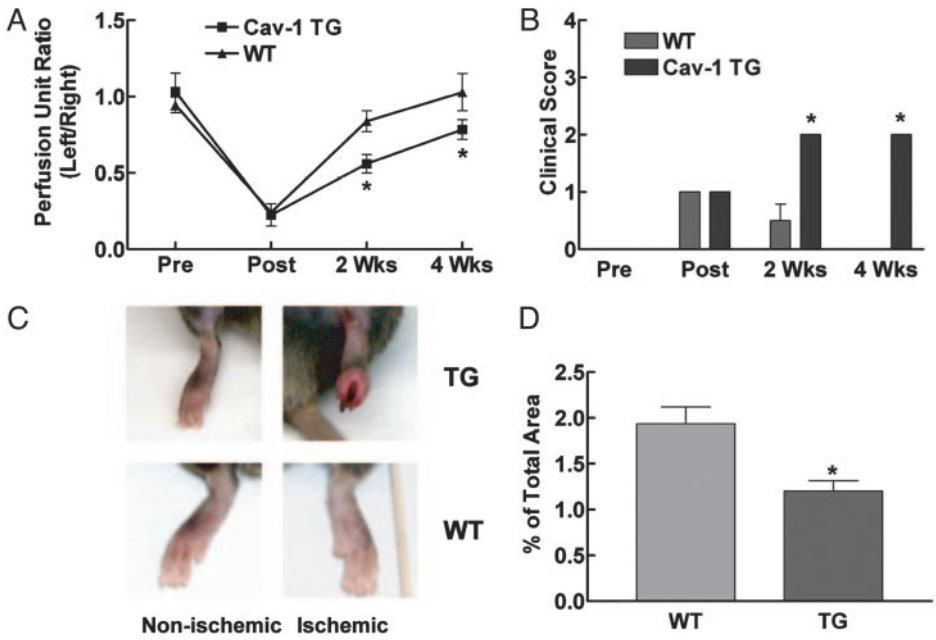

Fig. 5. Ischemia-induced arteriogenesis and angiogenesis are impaired in Cav-1 TG mice. (*A* and *B*) Arteriectomy was performed in Cav-1 TG and WT mice, and blood flow (*A*) and clinical index (*B*) were quantified over time. Data are mean ± SEM ($n = 6$). (*C*) The inflamed, necrotic foot seen in nonischemic (*Upper Left*) and ischemic (*Upper Right*) Cav-1 TG mice, compared with littermate controls (*Lower*). (*D*) The reduction in blood-flow recovery and clinical outcome were attributable to a decrease in lower-limb angiogenesis. Data are mean ± SEM, with $n = 6$ animals per group. Four fields per section and five sections per animal were quantified. *, $P < 0.05$.

of their foot due to the lack of blood flow, and this loss did not recover at the 4-week time point (Fig. 5*C*). Finally, we quantified the extent of angiogenesis in the lower limb by quantitative PECAM staining. As seen in Fig. 5*D*, there was a 35% decrease in PECAM-1-positive capillaries in the ischemic gastrocnemius muscle of the TG mice, compared with littermates, suggesting that the lack of blood flow recovery was due to defects in angiogenesis.

Our study using EC-specific Cav-1 TG mice raises several important questions regarding the regulation and functions of Cav-1 and caveolae *in vivo*. Surprisingly, despite clear phenotypes of TG expression on vascular functions (NO production, VEGF-stimulated permeability and angiogenesis, VEGF signaling, and ischemia-triggered angiogenesis), these results occur in the absence of obvious changes in caveolae number analyzed by quantitative EM. Our data suggest that the number of caveolae in the endothelium *in vivo* is not limited by the levels of Cav-1, as is typically seen in many cultured cell systems. Because fluid shear stress increases Cav-1 levels and caveolae number in cultured endothelial cells (34), perhaps the continual shear stress determined by blood flow *in vivo* maintains steady-state levels of caveolae *in vivo*. In addition, our data are consistent with results showing an increase in eNOS activation and leakiness of vessels in mice lacking Cav-1 and caveolae (30), because endothelial-specific expression of Cav-1 reduces eNOS activation, NO-dependent vascular function, and VEGF-stimulated permeability. However, our data differ from studies in Cav-1(−/−) mice that show decreased ischemia-induced angiogenesis (35), whereas in the present study, both VEGF-and ischemia-mediated angiogenesis are reduced by EC overexpression of Cav-1. The mechanism of impaired arteriogenesis/angiogenesis in Cav-1(−/−) mice appears also to be due to defective VEGFR signaling to ERK, Akt, and eNOS. Interestingly, the authors show *in vitro* that, both in Cav-1(−/−) endothelial cells and in endothelial cells reconstituted with higher levels of Cav-1, VEGF signaling is defective, although the mechanism for these effects is unclear. Perhaps in the Cav-1(−/−) mice, the loss of the caveolae organelle impairs spatial activation of the VEGFR, and in our study, the overexpression of Cav-1 does not influence organelle turnover but directly inhibits pathways downstream of the VEGFR receptor by a protein–protein interaction. The decreases in VEGF-mediated functions in Cav-1 TG mice were not due to changes in VEGFR2 tyrosine phosphorylation or coupling to ERK but occur through negative regulation of the PI-3K/Akt/eNOS signaling module, which diminishes the ability of VEGF to promote cell migration, organization, and NO production (36, 37). Indeed, in postnatal mice, eNOS is critical for the actions of exogenous VEGF and for ischemia-mediated arteriogenesis (33). Thus, the impaired VEGF permeability and angiogenesis is consistent with the established inhibitory action of Cav-1 on eNOS (38, 39) and tyrosine kinase-associated phosphatidylinositol 3-kinase activity (40). Our data strongly support the concept that Cav-1 can indeed regulate cellular functions through protein–protein interactions and provide an additional model to define the functionally relevant roles of Cav-1 in the endothelium, *in vivo*.

We thank Dr. Mitsuhiro Yokoyama (Kobe University School of Medicine, Kobe, Japan) for the PEP8 vector and Dr. Michael Lisanti (Albert Einstein College of Medicine, Bronx, NY) for the murine and canine Cav-1 cDNAs. This work was supported by National Institutes of Health Grants R01-HL64793, R01-HL 61371, R01-HL 57665, and P01-HL 70295; and National Heart, Lung, and Blood Institute–Yale Proteomics Contracts N01-HV-28186 (to W.C.S.) and F32 HL 072618-01 (to P.M.B.).

1. Bruns, R. R. & Palade, G. E. (1968) *J. Cell Biol.* **37,** 244–276.
2. Fielding, P. E. & Fielding, C. J. (1995) *Biochemistry* **34,** 14288–14292.
3. Smart, E. J., Ying, Y., Donzell, W. C. & Anderson, R. G. (1996) *J. Biol. Chem.* **271,** 29427–29435.
4. Schnitzer, J. E., Oh, P. & McIntosh, D. P. (1996) *Science* **274,** 239–242.
5. Anderson, R. G., Kamen, B. A., Rothberg, K. G. & Lacey, S. W. (1992) *Science* **255,** 410–411.
6. Kurzchalia, T. V. & Parton, R. G. (1999) *Curr. Opin. Cell Biol.* **11,** 424–431.
7. Lisanti, M. P., Scherer, P. E., Vidugiriene, J., Tang, Z., Hermanowski-Vosatka, A., Tu, Y. H., Cook, R. F. & Sargiacomo, M. (1994) *J. Cell Biol.* **126,** 111–126.
8. Okamoto, T., Schlegel, A., Scherer, P. E. & Lisanti, M. P. (1998) *J. Biol. Chem.* **273,** 5419–5422.
9. Shaul, P. W. & Anderson, R. G. (1998) *Am. J. Physiol.* **275,** L843–L851.
10. Drab, M., Verkade, P., Elger, M., Kasper, M., Lohn, M., Lauterbach, B., Menne, J., Lindschau, C., Mende, F., Luft, F. C., *et al.* (2001) *Science* **293,** 2449–2452.
11. Razani, B., Engelman, J. A., Wang, X. B., Schubert, W., Zhang, X. L., Marks, C. B., Macaluso, F., Russell, R. G., Li, M., Pestell, R. G., *et al.* (2001) *J. Biol. Chem.* **276,** 38121–38138.
12. Engelman, J. A., Chu, C., Lin, A., Jo, H., Ikezu, T., Okamoto, T., Kohtz, D. S. & Lisanti, M. P. (1998) *FEBS Lett.* **428,** 205–211.
13. Li, S., Okamoto, T., Chun, M., Sargiacomo, M., Casanova, J. E., Hansen, S. H., Nishimoto, I. & Lisanti, M. P. (1995) *J. Biol. Chem.* **270,** 15693–156701.
14. Garcia-Cardena, G., Fan, R., Stern, D. F., Liu, J. & Sessa, W. C. (1996) *J. Biol. Chem.* **271,** 27237–27240.
15. Frank, P. G., Lee, H., Park, D. S., Tandon, N. N., Scherer, P. E. & Lisanti, M. P. (2004) *Arterioscler. Thromb. Vasc. Biol.* **24,** 98–105.
16. Cohen, A. W., Razani, B., Wang, X. B., Combs, T. P., Williams, T. M., Scherer, P. E. & Lisanti, M. P. (2003) *Am. J. Physiol. Cell Physiol.* **285,** C222–C235.
17. Cohen, A. W., Park, D. S., Woodman, S. E., Williams, T. M., Chandra, M., Shirani, J., Pereira de Souza, A., Kitsis, R. N., Russell, R. G., Weiss, L. M., *et al.* (2003) *Am. J. Physiol. Cell Physiol.* **284,** C457–C474.
18. Ohashi, Y., Kawashima, S., Hirata, K., Yamashita, T., Ishida, T., Inoue, N., Sakoda, T., Kurihara, H., Yazaki, Y. & Yokoyama, M. (1998) *J. Clin. Invest.* **102,** 2061–2071.
19. Hungerford, J. E., Sessa, W. C. & Segal, S. S. (2000) *FASEB J.* **14,** 197–207.
20. Rebar, E. J., Huang, Y., Hickey, R., Nath, A. K., Meoli, D., Nath, S., Chen, B., Xu, L., Liang, Y., Jamieson, A. C., *et al.* (2002) *Nat. Med.* **8,** 1427–1432.
21. Vogel, U., Sandvig, K. & van Deurs, B. (1998) *J. Cell Sci.* **111,** 825–832.
22. Parolini, I., Sargiacomo, M., Galbiati, F., Rizzo, G., Grignani, F., Engelman, J. A., Okamoto, T., Ikezu, T., Scherer, P. E., Mora, R., *et al.* (1999) *J. Biol. Chem.* **274,** 25718–25725.
23. Lipardi, C., Mora, R., Colomer, V., Paladino, S., Nitsch, L., Rodriguez-Boulan, E. & Zurzolo, C. (1998) *J. Cell Biol.* **140,** 617–626.
24. Fra, A. M., Williamson, E., Simons, K. & Parton, R. G. (1995) *Proc. Natl. Acad. Sci. USA* **92,** 8655–8659.
25. Li, S., Song, K. S., Koh, S. S., Kikuchi, A. & Lisanti, M. P. (1996) *J. Biol. Chem.* **271,** 28647–28654.
26. Feron, O., Belhassen, L., Kobzik, L., Smith, T. W., Kelly, R. A. & Michel, T. (1996) *J. Biol. Chem.* **271,** 22810–22814.
27. Garcia-Cardena, G., Martasek, P., Masters, B. S., Skidd, P. M., Couet, J., Li, S., Lisanti, M. P. & Sessa, W. C. (1997) *J. Biol. Chem.* **272,** 25437–25440.
28. Scotland, R. S., Chauhan, S., Vallance, P. J. & Ahluwalia, A. (2001) *Hypertension* **38,** 833–839.
29. Huang, A., Sun, D., Smith, C. J., Connetta, J. A., Shesely, E. G., Koller, A. & Kaley, G. (2000) *Am. J. Physiol. Heart Circ. Physiol.* **278,** H762–H768.
30. Schubert, W., Frank, P. G., Woodman, S. E., Hyogo, H., Cohen, D. E., Chow, C. W. & Lisanti, M. P. (2002) *J. Biol. Chem.* **277,** 40091–40098.
31. Labrecque, L., Royal, I., Surprenant, D. S., Patterson, C., Gingras, D. & Beliveau, R. (2003) *Mol. Biol. Cell* **14,** 334–347.
32. Eliceiri, B. P., Paul, R., Schwartzberg, P. L., Hood, J. D., Leng, J. & Cheresh, D. A. (1999) *Mol. Cell* **4,** 915–924.
33. Murohara, T., Asahara, T., Silver, M., Bauters, C., Masuda, H., Kalka, C., Kearney, M., Chen, D., Symes, J. F., Fishman, M. C., *et al.* (1998) *J. Clin. Invest.* **101,** 2567–2578.
34. Boyd, N. L., Park, H., Yi, H., Boo, Y. C., Sorescu, G. P., Sykes, M. & Jo, H. (2003) *Am. J. Physiol. Heart Circ. Physiol.* **285,** H1113–H1122.
35. Sonveaux, P., Martinive, P., DeWever, J., Batova, Z., Daneau, G., Pelat, M., Ghisdal, P., Gregoire, V., Dessy, C., Balligand, J. L. & Feron, O. (2004) *Circ. Res.* **95**, 154–161.
36. Papapetropoulos, A., Garcia-Cardena, G., Madri, J. A. & Sessa, W. C. (1997) *J. Clin. Invest.* **100,** 3131–3139.
37. Ziche, M., Morbidelli, L., Choudhuri, R., Zhang, H. T., Donnini, S., Granger, H. J. & Bicknell, R. (1997) *J. Clin. Invest.* **99,** 2625–2634.
38. Bucci, M., Gratton, J. P., Rudic, R. D., Acevedo, L., Roviezzo, F., Cirino, G. & Sessa, W. C. (2000) *Nat. Med.* **6,** 1362–1367.
39. Gratton, J. P., Yu, J., Griffith, J. W., Babbitt, R. W., Scotland, R. S., Hickey, R., Giordano, F. J. & Sessa, W. C. (2003) *Nat. Med.* **9,** 357–362.
40. Zundel, W., Swiersz, L. M. & Giaccia, A. (2000) *Mol. Cell. Biol.* **20,** 1507–1514.